

Probabilistic Sampling of Balanced K-Means using Adiabatic Quantum Computing

Jan-Nico Zaech

Computer Vision Laboratory
ETH Zurich

jan-nico.zaeche@vision.ee.ethz.ch

Martin Danelljan

Computer Vision Laboratory
ETH Zurich

martin.danelljan@vision.ee.ethz.ch

Luc Van Gool

Computer Vision Laboratory, ETH Zurich
ESAT-PSI, KU Leuven
INSAIT

vangool@vision.ee.ethz.ch

Abstract

Adiabatic quantum computing (AQC) is a promising quantum computing approach for discrete and often NP-hard optimization problems. Current AQCs allow to implement problems of research interest, which has sparked the development of quantum representations for many computer vision tasks. Despite requiring multiple measurements from the noisy AQC, current approaches only utilize the best measurement, discarding information contained in the remaining ones. In this work, we explore the potential of using this information for probabilistic balanced k-means clustering. Instead of discarding non-optimal solutions, we propose to use them to compute calibrated posterior probabilities with little additional compute cost. This allows us to identify ambiguous solutions and data points, which we demonstrate on a D-Wave AQC on synthetic and real data.

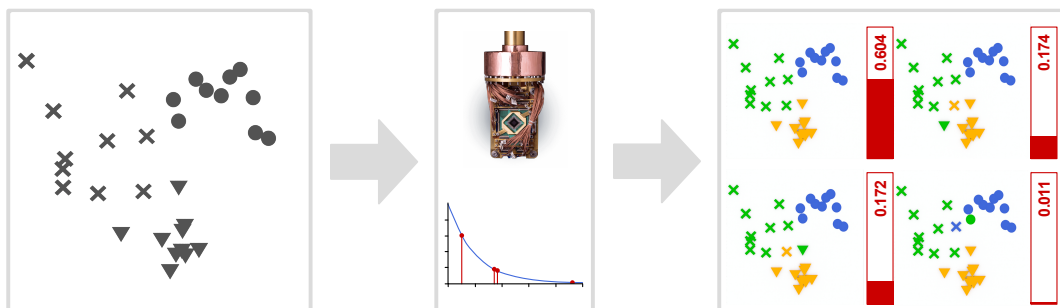


Figure 1: The proposed approach uses an adiabatic quantum computer to sample solutions of a balanced k-means problem. By using an energy-based formulation, likely solutions are drawn from a Boltzmann distribution. By reparametrizing the distribution, the calibrated posterior probability of each solution can be estimated.

1 Introduction

Clustering is a fundamental problem in machine learning and computer vision, extensively employed for the analysis and organization of large volumes of unlabeled visual data. It involves grouping similar objects based on their features, facilitating efficient data processing and unsupervised learning algorithms (Xu & Wunsch, 2005). The informa-

tion extracted from clusters plays a vital role in various computer vision applications, including image classification (Lazebnik et al., 2006; Caron et al., 2018), segmentation (Coleman & Andrews, 1979; Dhanachandra et al., 2015), tracking (Keuper et al., 2020), and network training (Coates & Ng, 2012; Yang et al., 2016). However, the often NP-hard computational complexity of solving clustering problems often hinders their application to large-scale problems that require fast processing times (Xu & Wunsch, 2005).

In addition to this, the ambiguity of the task itself contributes to the absence of a unique definition for clustering (Xu & Wunsch, 2005), which arises from the range of possible optimization objectives. An example of this are different algorithms that can optimize for the most compact solution, an underlying data-generating process or just use local distances. One way to address this challenge is the use of confidence-based estimators and the sampling of multiple likely solutions. This approach helps in identifying well-assigned samples and uncovering ambiguities within the data (Xu & Wunsch, 2005).

Quantum algorithms that promise a considerable speedup over their classical counterparts and are inherently probabilistic have the potential to enable a new family of machine learning algorithms. By now, quantum machine learning algorithms approach tasks such as optimization of quadratic problems (Kadowaki & Nishimori, 1998), training of restricted Boltzmann machines (Dixit et al., 2021), and learning with quantum neural networks (Abbas et al., 2021). While the current quantum computers can only solve small-scale problems, they provide the basis to develop and test algorithms that can considerably increase the size of feasible problems in the future.

In our work, we propose to exploit the probabilistic nature of a quantum computer to sample multiple high-probability solutions of the balanced k-means problem at little additional cost. By formulating the k-means objective as a quadratic energy function, we embed the clustering task into the quantum-physical system of an AQC. By repeatedly measuring the quantum system, we sample high-probability solutions according to the Boltzmann distribution. Unlike previous approaches that only use the best solution and discard all other measurements, we utilize all samples to generate probabilistic solutions for the k-means problem, as shown in Figure 1. We recalibrate the samples of the clustering problem to address temperature mismatch (Pochart et al., 2021), estimating the posterior probability for each solution, which allows us to identify ambiguous points and provides alternative solutions. We demonstrate the algorithm on a D-Wave quantum computer and perform extensive experiments in simulation. However, our primary objective is to explore the potential and efficient utilization of quantum computing for machine learning. The primary contributions of our work are as follows:

- We propose a quantum computing formulation of balanced k-means clustering that predicts well-calibrated confidence values and provides a set of alternative clustering solutions.
- A reparametrization approach is used to compute posterior probabilities from samples that avoids exact tuning of the AQC sampling temperature.
- Extensive experiments on synthetic and real data show the calibration of our approach using simulation as well as the D-Wave Advantage 2 AQC prototype.

2 Related Work

With the availability of quantum computers to the general research community (Bunyk et al., 2014; McGeoch & Farré, 2021; McGeoch et al., 2022; Debnath et al., 2016), the research interest in finding applications for such systems has considerably increased. In this context AQC (Kadowaki & Nishimori, 1998; Bunyk et al., 2014) provides a well-tangible starting point, even though many applications need a complete reformulation considering the architectural differences of a quantum computer. Current applications for AQC include solving optimization problems for improved traffic flow (Neukart et al., 2017), robotic routing problems (Ohzeki et al., 2019), the design of molecules (Mulligan et al., 2020) or portfolio optimization in the finance sector (Mugel et al., 2021). Recently, the computer vision community has developed a strong interest in finding applications for quantum computing, which are related to hard permutation problems (Birdal et al., 2021) like tracking (Zaech et al., 2022) and graph-matching (Benkner et al., 2021).

Clustering is a well-studied problem for quantum- as well as quantum-inspired algorithms (Aïmeur et al., 2007). Quantum clustering (Horn & Gottlieb, 2001) uses the Schrödinger equation to model the clustering problem, where cluster centers are defined as the minima of the corresponding potential function. Casaña-Eslava et al. (2020) extend this formulation with a probabilistic estimate of cluster memberships. These approaches use classical computation and gate-based quantum computers that are currently still on a small scale.

Closest to this work, Arthur & Date (2021) present a balanced k-means clustering algorithm suitable for an AQC. While our underlying clustering algorithm follows the same approach, Arthur & Date (2021) discard all but the best measurement. Our approach, however, utilizes all information by employing AQC as a sampler to generate probabilistic solutions of the clustering problem, rather than only using the best solution in an optimization framework.

3 Theory

3.1 Quantum Computing

Quantum computing is a fundamentally new approach, that utilizes the state of a quantum system to perform computations. In contrast to a classical computer, the state is probabilistic and described by its wave function, which enables the use fundamental properties of quantum systems like superposition and entanglement. Quantum algorithms that can efficiently run on these systems allow to solve previously infeasible problems, including the well-known prime factorization by Shor’s algorithm (Shor, 1999). In the following, the most important basics of quantum computing are explained.

Qubit. The qubit forms the basic building block of a quantum computer. In contrast to the classical bit, which is always in either of its two basis states $|0\rangle, |1\rangle$, the qubit can exist in a state of superposition, which is a linear combination of any two basis states

$$|\psi\rangle = \alpha |0\rangle + \beta |1\rangle. \quad (1)$$

The two complex-valued factors α, β describing the superposition are called amplitudes.

Entanglement. To perform meaningful operations, a quantum computer operates on a system of multiple qubits. If the qubits are independent of each other, the joint state of the system can be computed as the tensor-product of all involved qubit states. If the qubits of a system are entangled (Einstein et al., 1935; Schrödinger, 1935), it is not possible to decompose the joint state into the tensor-product of each separate qubit state. Therefore, measuring the state of one qubit in a entangled system, affects the state of the other qubits. This is a fundamental property of quantum mechanics and plays a crucial role for the capabilities of quantum computing.

Measurement. During computation on the quantum computer, the state of the system can be any valid superposition of basis states. Nevertheless a measurement of the system always results in a single basis state, which is referred to as wave-function collapse (Wilde, 2017). The probability of measuring a state is the respective squared amplitude. In the single qubit case as described in equation 1, this corresponds to

$$p(|0\rangle) = |\alpha|^2 \quad p(|1\rangle) = |\beta|^2. \quad (2)$$

In contrast to all other operations in quantum computing, this is not reversible.

3.2 Adiabatic Quantum Computing.

AQC, which is used in this work, is a quantum computing paradigm where the state of a quantum system is modified by performing an adiabatic transition. Current hardware implementations such as the D-wave systems (Bunyk et al., 2014) follow this approach and implement a Quantum Annealer (QA) to solve quadratic unconstrained binary optimization (QUBO). They are based on the Ising model (Ising, 1925; Kadowaki & Nishimori, 1998), which describes the configuration of a set of interacting particles that all carry an atomic spin σ_i .

The spin can either be +1 or -1 and the particles are coupled by interactions J_{ij} as well as influenced individually by a transversal magnetic field h_i . The energy of this system is described by its Hamiltonian function

$$H(\sigma) = - \sum_i \sum_j J_{ij} \sigma_i \sigma_j - \sum_i h_i \sigma_i. \quad (3)$$

Thus, finding the lowest energy state or ground state of the Ising model corresponds to solving the QUBO defined by the Hamiltonian function. This relation is used in the QA, where the system of qubits implements an Ising model H_T that represents the QUBO of interest.

The lowest energy state is found by following the adiabatic theorem (Born & Fock, 1928). Starting with an initial system in its ground state described by an Hamiltonian H_0 , the adiabatic theorem states that during a sufficiently slow change of the Hamiltonian the system never leaves its ground state. The change of the Hamiltonian

$$H(t) = H_0(1 - \frac{t}{T_a}) + H_T \frac{t}{T_a} \quad (4)$$

is called an adiabatic transition. The transition is performed over the annealing-time T_a and allows to solve an optimization problem with the Hamiltonian H_T .

While in an ideal noise-free case, the system stays in its ground state, any real system is embedded in a temperature bath that can induce a change to a higher energy state. The distribution of measured final states will then follow the Boltzmann distribution with temperature T

$$p(\sigma) = \frac{\exp[-H(\sigma)/T]}{\sum_{\sigma'} \exp[-H(\sigma')/T]}, \quad (5)$$

where $p(\sigma)$ describes the probability of finding the system in state σ and σ' are all possible states. In this work, we use this property, as it allows us to sample from the Boltzmann distribution corresponding to the energy-based model of clustering.

3.3 Energy-Based Models

Energy-based models are probabilistic models that use an energy function $E(\mathbf{x})$ to describe the probability of each system state. By assigning an energy value to each system state, the probabilities are Boltzmann distributed

$$p(\mathbf{x}) = \frac{1}{A} \exp[E(\mathbf{x})/T], \quad (6)$$

with the temperature T as a free parameter in this model and the normalization constant A ensuring that the values are valid probabilities. Our model follows this approach and represents the clustering problem as an energy-based formulation.

One challenging task to use energy-based models remains in sampling the system according to the Boltzmann distribution as this is NP-hard for the quadratic Ising-model formulation (Pochart et al., 2021). While this is usually approximated on classical hardware with the corresponding computational overhead, AQC provides a direct way to sample from a physical system that follows the Boltzmann distribution (Pochart et al., 2021).

3.4 Clustering

Clustering is one core task required in many unsupervised machine learning algorithms. It has the objective to group a set of points \mathbf{X} into disjoint clusters $\{c_1, \dots, c_K\}$, where each cluster contains points that are similar in the feature space. A design parameter is the definition of the similarity metric, which leads to a wide range of clustering algorithms available. The popular and simple k-means algorithm (Forgy, 1965; Lloyd, 1982) optimizes the quadratic distance to a centroid. Such distance-based metrics assume clusters to be compact, while other approaches such as dbscan (Ester et al., 1996) define features as similar if they come from a contiguous region of high density.

In this work, balanced clustering is investigated, where a defined target cluster size s_k is required. This approach forms the basis of many AQC-based algorithms (Benkner et al., 2020; Birdal et al., 2021; Zaech et al., 2022) and has a wide range of further applications such as secret key generation in cryptography (Hong et al., 2017), energy-efficient data aggregation in wireless sensor networks (Liao et al., 2013), or data cleaning (Fisher et al., 2015).

Uncertainty estimation in clustering and machine learning aims at quantifying the confidence that predictions made by a model correspond to the underlying ground-truth. The confidence scores can be used to eliminate uncertain samples from the solution, to select a set of possible hypotheses or to find the right parameters of the algorithm itself (Casaña-Eslava et al., 2019).

Uncertainty estimates can be generated separately for each data-point by evaluating the likelihood function $p(\mathbf{X}|\hat{\mathbf{Z}})$, or by computing the posterior probability $p(\hat{\mathbf{Z}}|\mathbf{X})$ that describes the probability of the whole clustering solution. As the

former can be evaluated if the data generating model is defined, it can be combined with most clustering approaches. Nevertheless, as the likelihood function is not a probability distribution of the cluster assignments, it does not provide a calibrated prediction. In contrast to this, the posterior probability $p(\mathbf{Z}|\mathbf{X})$ directly represents the probability that the estimated assignment \mathbf{Z} corresponds to the ground-truth. While this provides an interpretable result, it is often infeasible to compute as all possible assignments need to be evaluated in order to find the normalizing constant.

The set of possible clustering solutions together with their posterior probabilities provides valuable information that can be utilized for a range of low- as well as high-level reasoning tasks. On a low level, the probability of the best solutions can be used to identify the right number of clusters. If a number different than the number of the data-generating process is chosen, additional ambiguity is introduced. For a larger number during clustering than present in the data, the strong overlap between the corresponding distributions induces high ambiguity, while an insufficient number of clusters spreads points inside a single cluster far apart, which reduces the associated probability.

For high-level applications, calibrated samples of possible clustering solutions can provide additional information in multi-object tracking (Chiu et al., 2021). Following the AQC framework, tracking can be implemented as a clustering problem with additional constraints that represent the temporal relation between points (Zaech et al., 2022). Each cluster then corresponds to one object in the video, with each point representing it at a different timestep. The feature used to define clusters can either be visual similarity from re-identification (Hirzer et al., 2011; Paisitkriangkrai et al., 2015; Zheng et al., 2019) features or spatial similarity (Bewley et al., 2016). Different solutions thus represent different tracks through time, where ambiguities can be generated by occlusions or crossing paths. In a larger system such as an autonomous vehicle, knowing all likely candidate solutions can allow for predicting multimodal candidates for future trajectories (Jiang et al., 2023; Deo & Trivedi, 2018) and can help to evaluate the risk of taking any action. In a similar approach, feature matching can be formulated (Birdal et al., 2021) and ambiguous candidates can be discarded during 3d reconstruction or camera pose estimation.

3.5 Clustering as QUBO

To solve the clustering problem using AQC, a QUBO formulation is required. We use a variation of the one-hot encoding approach (Date et al., 2021; Arthur & Date, 2021) that uses a matrix $Z \in \{0, 1\}^{K \times I}$ to encode the cluster assignment of I samples to K clusters. Each row corresponds to one of K clusters and each column to one of I samples. An entry $Z_{ki} = 1$ indicates that the sample x_i belongs to cluster c_k .

As each sample needs to be assigned to a single cluster, the sum of each column of Z needs to satisfy the constraint $\sum_k Z_{ki} = 1 \forall i$. The implementation of constrained clustering, where each cluster has a fixed size s_k furthermore requires the row constraints $\sum_i Z_{ki} = s_k \forall k$ on Z .

With the cost $q(i, j, k)$ for assigning the pair of samples x_i and x_j to the same cluster c_k , the optimization problem reads

$$\begin{aligned} \hat{Z} &= \arg \min_Z \sum_k \sum_i \sum_j Z_{ki} Z_{kj} q(i, j, k) \\ \text{s.t. } &\sum_k Z_{ki} = 1 \forall i \quad \wedge \quad \sum_i Z_{ki} = s_k \forall k. \end{aligned} \tag{7}$$

By vectorizing Z in row-major order as $\mathbf{z} = \text{vec}(Z)$, the optimization problem can be rewritten in matrix form as

$$\hat{\mathbf{z}} = \arg \min_{\mathbf{z}} \mathbf{z}^T \mathbf{Q} \mathbf{z} \quad \text{s.t.} \quad \mathbf{G} \mathbf{z} = \mathbf{d}, \tag{8}$$

where \mathbf{Q} is a block diagonal matrix with blocks $\mathbf{Q}_0, \dots, \mathbf{Q}_K$ and $\mathbf{G} \mathbf{z} = \mathbf{d}$ corresponds to the matrix formulation of the constraints. Each block \mathbf{Q}_k of the cost matrix is a square matrix that contains the costs $q(i, j, k)$ at $\mathbf{Q}_{k, ij}$.

While the constraints are not directly covered by the QUBO problem, they can be modeled using Lagrangian multipliers. To avoid a mixed discrete and continuous optimization problem, a quadratic penalty reformulation $\lambda \|\mathbf{G} \mathbf{x} - \mathbf{d}\|_2^2$ is chosen, leading to the minimization problem

$$\hat{\mathbf{z}} = \arg \min_{\mathbf{z}} \mathbf{z}^T \mathbf{Q}' \mathbf{z} + \mathbf{b}'^T \mathbf{z} \tag{9}$$

with

$$\mathbf{Q}' = \mathbf{Q} + \lambda \mathbf{G}^\top \mathbf{G} \quad (10)$$

$$\mathbf{b}' = -2\lambda \mathbf{G}^\top \mathbf{b}. \quad (11)$$

In contrast to a linear penalty approach, where the multiplier λ needs to be optimized, our selection only requires a sufficiently high λ , as all constraint violations result in an increased penalty term. With such selection, the penalty term evaluates to zero $\lambda \|\mathbf{G}\mathbf{x} - \mathbf{d}\|_2^2 = 0$ if all constraints are fulfilled, and thus, the minimizer $\hat{\mathbf{z}}$ of the modified optimization problem is a minimizer of the original optimization problem in Equation equation 8.

Besides modeling balanced clustering, further constraints can be introduced using Lagrangian multipliers. This allows to represent a wide range of tasks as QUBO clustering problems solvable with AQC.

4 Probabilistic Quantum Clustering

4.1 Motivation

Our clustering formulation employs a mixture of Gaussians to explain the observations, where the cluster assignments are latent variables. Each sample in a cluster c_k is modeled as a sample drawn from a Gaussian distribution $\mathcal{N}(\mu_k, \mathbf{I})$ with mean μ_k and identity covariance according to the k-means setting. Following a Bayesian approach, the best clustering solution can be found by maximizing the posterior probability over possible assignments Z of points to clusters.

$$p(Z|\mathbf{X}) = \frac{p(\mathbf{X}|Z)p(Z)}{\sum_{Z'} p(\mathbf{X}|Z')} = \frac{p(\mathbf{X}|Z)p(Z)}{A}. \quad (12)$$

While this approach provides a probabilistic estimate by jointly modeling information about the possible cluster configurations and the distribution of data points, it is often intractable to evaluate due to the partitioning function $A = \sum_{Z'} p(\mathbf{X}|Z')$. Computing A requires to sum over all possible solutions Z , which grows exponentially with the number of samples in the clustering problem. To overcome this, we utilize an AQC that samples directly from a Boltzmann distribution, which we parameterize according to the probabilistic clustering problem.

4.2 Data Model

Determining the cost function of the optimization problem is a design choice of the algorithm. For our probabilistic approach, a well-defined data distribution, that forms the basis of the cost function is required. While many tasks approached in quantum computer vision, such as tracking (Zaech et al., 2022) or synchronization (Benkner et al., 2021; Birdal et al., 2021), costs are based on learned metrics or heuristics, they can also be trained to reflect the properties required in our approach.

We therefore, follow the mixture of Gaussian model, where each cluster generates samples from a normal distribution. With the independence of observations and clusters, given the distribution parameters, the likelihood of the joint observations for an assignment Z is given as the product of the individual likelihoods

$$f(\mathbf{X}|Z) = \prod_{k=1}^K f(\mathbf{X}|Z_k) = \prod_{k=1}^K \prod_{i \in Z_k} f(\mathbf{x}_i|Z_k) = \quad (13)$$

$$\prod_{k=1}^K \prod_{i \in Z_k} \frac{1}{\sqrt{2\pi^d}} \exp \left[-\frac{1}{2} (\mathbf{x}_i - \mu_k)^\top \mathbf{I} (\mathbf{x}_i - \mu_k) \right] = \quad (14)$$

$$\frac{1}{\sqrt{2\pi^d}} \exp \left[-\sum_{k=1}^K \sum_{i \in Z_k} \frac{1}{2} (\mathbf{x}_i - \mu_k)^\top \mathbf{I} (\mathbf{x}_i - \mu_k) \right] \quad (15)$$

where the likelihood $f(\mathbf{x}_i|Z_k)$ corresponds to a Gaussian distribution that follows $\mathcal{N}(\mu_k, \mathbf{I})$ and d is the dimensionality of the space. This result can be used to formulate the energy-based model with the energy function

$$E(\mathbf{X}|Z) = \sum_{k=1}^K \sum_{i \in Z_k} \frac{1}{2} (\mathbf{x}_i - \mu_k)^\top \mathbf{I} (\mathbf{x}_i - \mu_k). \quad (16)$$

Using the energy function to rewrite the posterior distribution leads to the Boltzmann distribution from Equation 5

$$p(Z|\mathbf{X}) = \frac{\exp[-(E(\mathbf{X}|Z) + E(Z))]}{\sum_{Z'} \exp[-E(\mathbf{X}|Z')]} \quad (17)$$

In this formulation, the energy of the assignment $E(Z)$ corresponds to the prior $p(Z)$, which models feasible and infeasible solutions by an indicator function. In the case of balanced clustering, this corresponds to allowing assignments that have each point assigned to exactly one cluster and a cluster size according to s_k .

Searching the most likely clustering solution corresponds to finding lowest energy solution on the AQC, as well as to the Maximum-a-Posteriori \hat{Z}_{map} estimate of the assignment

$$\hat{Z}_{\text{map}} = \arg \max_Z p(Z|\mathbf{X})p(Z) = \arg \min_Z E(\mathbf{X}|Z) + E(Z). \quad (18)$$

As the AQC qubit system is an Ising model, it requires formulating $E(\mathbf{X}|Z)$ and $E(Z)$ quadratic in the optimization variables Z , enabling the joint discovery of assignments and cluster means. This is achieved by using the maximum likelihood estimator of the mean, resulting in a quadratic energy formulation that fits the Ising model in Equation 9

$$E_k(\mathbf{X}|Z) = \frac{1}{s_k} \sum_i \sum_j Z_{ki} Z_{kj} (\mathbf{x}_i - \mathbf{x}_j)^\top (\mathbf{x}_i - \mathbf{x}_j). \quad (19)$$

The second energy term $E(Z)$ in Equation 17, modeling the prior distribution over possible assignments cannot exactly be embedded in the Ising model. We therefore use the quadratic penalty method as shown in Equation 9 to approximate the energy of an indicator function. Importantly, this does not influence the energy of feasible solutions, as $\lambda \|\mathbf{G}\mathbf{x} - \mathbf{d}\|_2^2$ evaluates to zero for all solutions that fulfill the clustering constraints.

4.3 Boltzmann Reparametrization

While ideally the measurements on AQC are direct samples from the Boltzmann distribution (D-Wave Systems Inc., 2017; Dixit et al., 2021), it requires solving a range of challenges that prohibit a direct use in our scenario (Pochart et al., 2021): Mapping between the cost function and the physical system implemented on the AQC requires Hamiltonian scaling (Pochart et al., 2021). Estimating the scaling factor is nontrivial (Nelson et al., 2022) and prohibitive for using samples directly in many cases. Additionally, hardware limitations including imperfection of the processor and the spin-bath polarization effect (Pochart et al., 2021) prevent the AQC to sample the Boltzmann distribution exactly. Finally, as the energy term $E(Z)$ can only be implemented using the penalty method, the sampling density is influenced by solutions not fulfilling the constraints.

We compensate for these limitations by evaluating the energy of all measured feasible solutions Z' and recompute $p(Z|\mathbf{X})$ by evaluating the partitioning function over these, which only requires sampling solutions at a sufficiently high temperature.

4.4 Maximum Pointsets

Having the set of the most likely clustering solutions Z available together with their posterior probability $P(Z|\mathbf{X})$ allows to find an assignment Z^* of a subset of points that solves the clustering problem with increased probability $P(Z^*|\mathbf{X})$. Such a set can be found by using Algorithm 1, which implements a greedy approach that disregards points that disagree between different clustering solutions.

In the case of a sufficiently well sampled Boltzmann distribution, the resulting maxset assignment Z^* with the corresponding probabilistic estimate $P(Z^*|\mathbf{X})$ is still calibrated.

Algorithm 1 MaxsetSearch

```
1:  $Z^* \leftarrow Z_0$ 
2:  $p \leftarrow P(Z_0|\mathbf{X})$ 
3:  $i \leftarrow 1$ 
4: while  $p \leq p_{\min}$  do
5:    $Z'_i \leftarrow \text{align}(Z_i, Z^*)$ 
    $\triangleright$  Find the cluster permutation that minimizes the number of points assigned to different clusters in  $Z_i$  and  $Z^*$ .
6:    $Z^* \leftarrow Z^* \cap Z'_i$ 
    $\triangleright$  Remove points assigned to different clusters.
7:    $p \leftarrow p + P(Z_i|\mathbf{X})$ 
8:    $i \leftarrow i + 1$ 
9: end while
10: return  $Z^*$ 
```

4.5 Inference Parameter Optimization

Using the quadratic penalty method to implement the constraints requires finding suitable Lagrangian multipliers λ . Even though a very high multiplier theoretically guarantees finding a feasible solution, it also deteriorates the conditioning of the optimization problem. Therefore, a suitable Lagrangian multiplier lifts the cost of any constraint violation above all relevant solutions of the clustering problem, while keeping them low enough to avoid scaling the total energy of the problem up considerably. To estimate the multipliers, we follow an iterative procedure as also proposed in (Zaech et al., 2022).

In an initial step, balanced k-means (Malinen & Fränti, 2014) is used to find a feasible clustering solution. This solution is used to estimate Lagrangian multipliers that avoid any first-order violation of the constraints. In subsequent iterative optimization steps, the problem is solved in simulation, to find multipliers that result in a well conditioned problem.

Such optimization procedure is crucial due to the low fidelity of the current generation of AQCs, which requires careful engineering of the problem energy. Therefore, we expect this procedure to become of reduced importance with the progress of quantum computing.

5 Experiments and Results

We perform experiments on synthetic data as well as real data to verify the efficacy of our method in finding the set of high-probability solutions and in estimating calibrated confidence scores. The experimental scenarios are solved with QA, Simulated Annealing (SIM), and exact exhaustive search using the presented energy formulation and with k-means as a baseline method, which all optimize for the same cost objective. This further allows us to understand the limitations and required work when deploying the approach to real quantum computers.

5.1 Solver Methods

Quantum annealing (QA) experiments are performed on the D-Wave Advantage 2 Prototype 1.1 (McGeoch et al., 2022). The system offers 563 working qubits, each connected with up to 20 neighbors. For each clustering problem 5000 measurements are performed, each with $50\mu\text{s}$ annealing time.

Due to the strong compute-time limitations on an AQC, all Lagrangian optimization steps are performed with SIM, before measuring the final results on the AQC.

Simulated annealing (SIM) provided by D-Wave is used for larger scale comparisons. Similar to QA, we perform 5000 runs for each clustering problem. We reduce the number of sweeps performed in each run to 30, which allows us to sample the Boltzmann distribution at a sufficiently high temperature in most scenarios, making it comparable to QA.

Solver Method	Accuracy	Completeness	Adjusted Rand Index	Fowlkes-Mallows Score	Accuracy	Completeness	Adjusted Rand Index	Fowlkes-Mallows Score	Accuracy	Completeness	Adjusted Rand Index	Fowlkes-Mallows Score		
	15 Points, 3 Clusters, 2 Dim					30 Points, 3 Clusters, 2 Dim					45 Points, 3 Clusters, 2 Dim			
SIM	56.4 ±1.6	79.5 ±0.8	74.7 ±1.0	81.9 ±0.7	38.6 ±1.5	74.2 ±0.8	73.3 ±0.9	81.6 ±0.6	50.8±1.6	86.2 ±0.5	87.3 ±0.5	91.4 ±0.3		
K-means	51.3±1.6	75.0±0.9	68.8±1.1	77.7±0.8	37.0±1.5	71.9±0.8	70.2±0.9	79.4±0.6	52.8 ±1.1	85.9±0.4	86.6±0.4	90.9±0.3		
	15 Points, 3 Clusters, 2 Dim					10 Points, 2 Clusters, 2 Dim					20 Points, 4 Clusters, 4 Dim			
QA	56.1±1.6	79.4±0.8	74.6±1.0	81.9 ±0.7	74.3 ±1.4	80.2 ±1.1	79.6 ±1.1	88.7 ±0.6	12.4±1.0	51.2±0.8	34.0±1.0	47.9±0.8		
SIM	56.4 ±1.6	79.5 ±0.8	74.7 ±1.0	81.9 ±0.7	74.1±1.4	80.0±1.1	79.5±1.1	88.6±0.6	32.4 ±1.5	70.4 ±0.8	59.2 ±1.1	67.8 ±0.8		
K-means	51.3±1.6	75.0±0.9	68.8±1.1	77.7±0.8	70.1±1.4	76.3±1.2	75.4±1.2	86.3±0.7	20.9±1.3	61.9±0.8	47.4±1.0	58.5±0.8		
Exhaustive	56.4 ±1.6	79.5 ±0.8	74.7 ±1.0	81.9 ±0.7	74.3 ±1.4	80.2 ±1.1	79.6 ±1.1	88.7 ±0.6	-	-	-	-		

Table 1: Synthetic data results for our approach (QA, SIM, exhaustive) and k-means. All numbers in % with standard error of the mean.

Exact exhaustive search is used as a reference method to validate the energy-based formulation on small problems. By iterating all feasible solutions, the lowest energy solution is guaranteed to be found and the partitioning function is computed exactly.

K-Means clustering with a balanced cluster constraint (Malinen & Fränti, 2014) forms the baseline for our approach. We run the algorithm until convergence for a maximum of 1000 iterations. While this solution does not provide a probabilistic estimate, it is useful to assess the relative clustering performance.

5.2 Dataset and Metrics

Data for the quantitative evaluation of our method is synthetically generated. For each clustering problem a total of I points are sampled from a separate normal distribution for each of K clusters. The cluster centers are randomly drawn, such that the distance between each pair of clusters lies within a predefined range $[d_{\min}, d_{\max}]$. For each experiment a total of L clustering tasks is generated. This allows us to evaluate the calibration metrics over a large value range. For all experiments that directly compare methods, identical clustering tasks are used.

Further qualitative examples are provided for the IRIS dataset (Fisher, 1936), which contains 50 samples of 4 features in 3 classes. We randomly subsample the points and dimensions to generate the parameters required for our experiments.

Clustering metrics are computed using the available ground-truth clusters. We evaluate 4 standard metrics: The accuracy, which measures the ratio of clustering solutions that are identical to the ground-truth. Completeness (Rosenberg & Hirschberg, 2007) measures the ratio of points from a single cluster being grouped together. The adjusted Rand score (Hubert & Arabie, 1985) compares all pairs of points in the ground truth and prediction and the Fowlkes-Mallows index (Fowlkes & Mallows, 1983) combines precision and recall into a single score.

5.3 Calibration Performance

We evaluate the calibration of our method on a synthetic clustering scenario with 3 clusters and 15 points using QA, SIM and exhaustive search on 1000 tasks. First all clustering solutions Z are accumulated in bins according to their estimated posterior probability $P(Z|X)$. This process also includes all sampled non-optimal but feasible solutions. The resulting histogram of solutions is shown in Figure 2a. After accumulation, the ratio of correct solutions in each bin is evaluated in Figures 2b, 2c, and 2d, which for a calibrated method should be close to the mean predicted probability represented by the diagonal. We find our approach to generate well-calibrated probabilities in both simulation and when using QA.

5.4 Clustering Performance

We evaluate the performance of our clustering formulation using synthetic data in Table 1. The upper rows show results for 3 clusters with an increasing number of points and 1000 tasks/setting for SIM and k-means. Due to the problem size, results cannot be found using QA and exhaustive search. Comparing results shows that most clustering metrics are better when using our formulation with SIM, however, the difference decreases with increasing problem

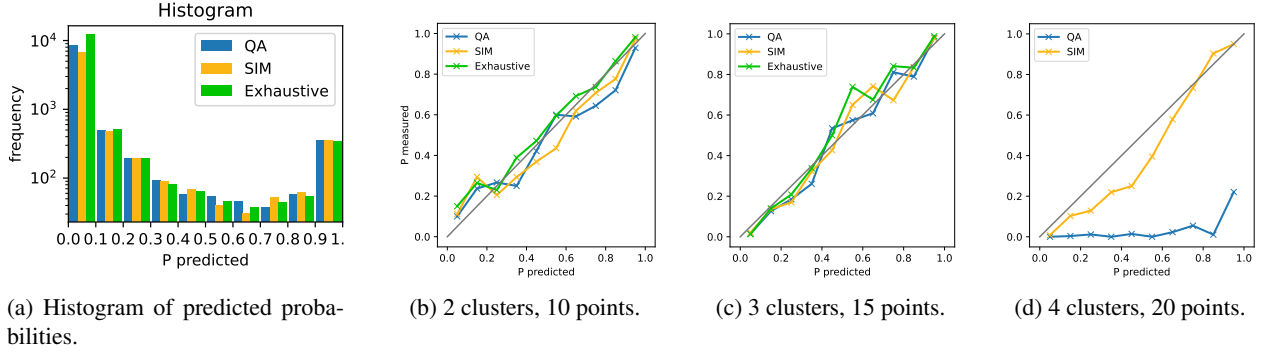


Figure 2: Evaluation of the calibration for QA, SIM and exhaustive search in a clustering scenario with 15 points and 3 clusters. Evaluation of the calibration for quantum annealing, simulated annealing and exhaustive search in clustering scenarios with 2, 3, and 4 clusters and 5 points in each cluster. All results are generated with 1,000 problems in each scenario and 5,000 measurements for each clustering problem.

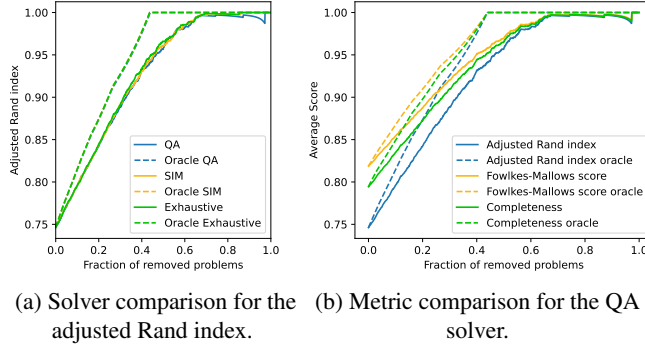


Figure 3: Sparsification plots of clustering metrics.

size. This can be attributed to the globally optimal solution our approach is optimizing for. While in an ideal the global solution is at least as good as the k-means solution, an increasing problem size also increases the complexity of the corresponding QUBO. This makes it harder to solve exactly and the noisy approach using annealing is not capable of solving the problem correctly.

For the largest clustering problem with 3 clusters and 45 points, k-means provides the best accuracy and thus, a larger number of correct solutions compared to SIM. However, the metrics indicating clustering quality are higher for SIM. This indicates that our formulation is able to find a better solution in cases where the problem is not solved correctly by SIM and k-means.

The lower rows in Table 1 show settings with 2,3, and 4 clusters, each containing 5 points, again with 1000 tasks/setting. For the two smaller scenarios QA on the D-wave Advantage 2 provides results close or identical to SIM and exhaustive search. For the largest scenario with 20 points in 4 clusters, QA loses performance.

The quality of predicted posterior probabilities can be further evaluated by linking them to the clustering metrics and sparsifying the set of tasks. Starting with metrics over the whole set of clustering tasks, we remove tasks according to increasing predicted probability and evaluate the metric over the remaining set. In an ideal predictor, this removes the lowest performing tasks first. In Figures 3a and 3b this is done for the adjusted Rand index with different solvers and for QA with different metrics respectively. The solid lines show the sparsification-plots using the predicted probabilities and the dashed lines show the same plots for an oracle method that generates the best possible ordering based on the metrics themselves.

In Figure 3a it becomes apparent that QA, SIM and exhaustive search perform close to each other over most of the value range. Nevertheless, for a high sparsification with more than 80% of the tasks removed, QA shows a drop in

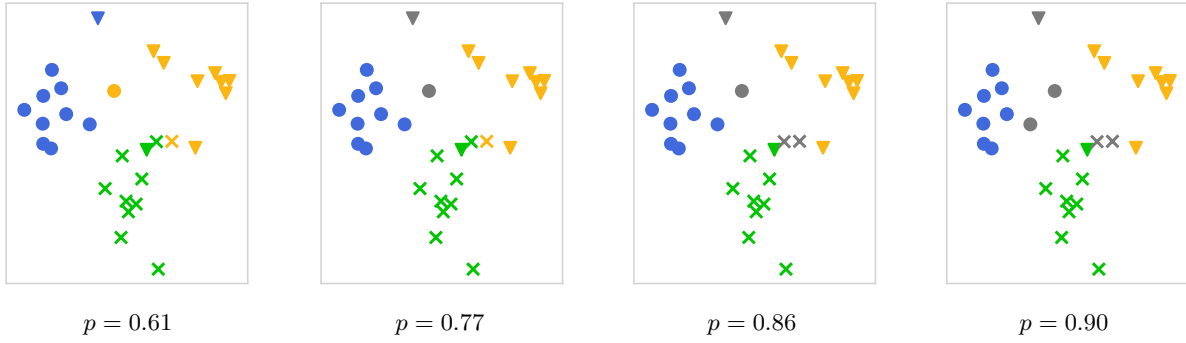


Figure 4: Visualization of max pointsets for synthetic data with the probability for each of the determined pointsets.

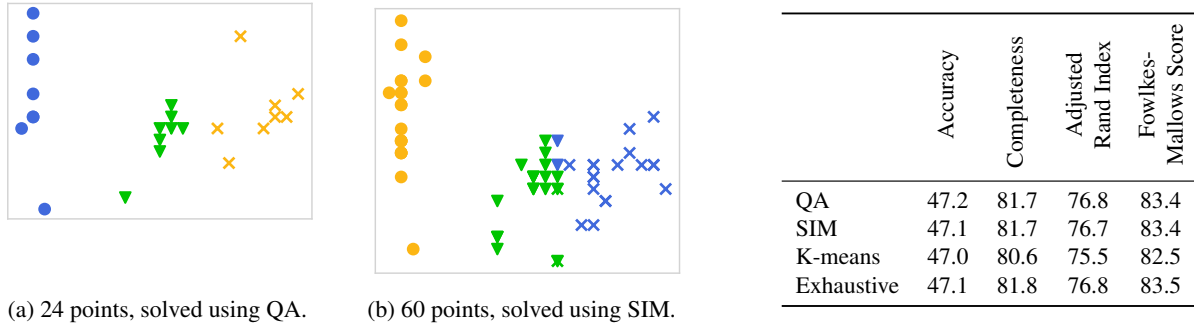


Figure 5: Qualitative results on the IRIS dataset.

Table 2: Clustering metrics generated on IRIS subsets using 3 clusters with 15 points in total.

performance compared to the other methods. This is caused by tasks where only a single, but incorrect solution is found, which gets assigned a posterior probability of $P(Z|\mathbf{X}) = 1.0$. In such cases the Boltzmann distribution has not been sampled sufficiently well, either because of too few measurements or because of a low effective sampling temperature. As SIM does not show this behavior the source can likely be traced back to current limitation of the quantum computer.

5.5 Maximum Pointsets

Qualitative examples for the maximum pointsets generated with Algorithm 1 are depicted in Figure 4. The shape of each point represents the ground truth class and the color the assigned cluster. Starting with the most likely solution having a predicted probability of $p(Y|X) = 0.61$ on the left, each plot shows one additional step of the algorithm, which successively removes points from the solution, indicated by plotting them in Grey. The illustration demonstrates that the MaxsetSearch algorithm is able to generate well-separated clusters from the probabilistic predictions.

5.6 IRIS Dataset

While our method assumes an identity covariance in the data, it can be applied to other distributions, which we evaluate on the widely used IRIS dataset. Clustering metrics for experiments using 3 clusters with 5 points each are provided in Table 2 and show that our formulation using QA and SIM is competitive with k-means. Figures 5a and 5b show differently sized qualitative examples from the dataset solved using our formulation with QA and SIM respectively.

Though the value of the predicted probability cannot be interpreted easily with the mismatch between the assumed and the actual data-generating process, it can be used to find maximum pointsets. The results from Algorithm 1 using results from SIM are provided in Figure 6 and show that even for a distribution mismatch the maximum pointsets can provide meaningful results for removing ambiguous samples.

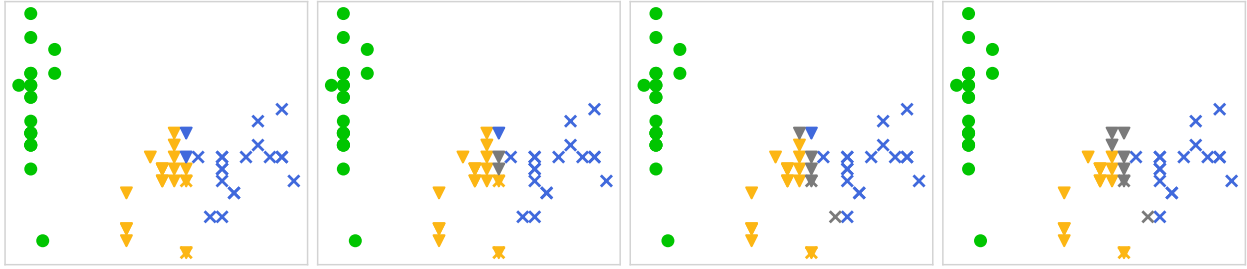


Figure 6: Max pointsets generated using simulated annealing on the IRIS dataset with 60 points.

6 Conclusion

In this work, we proposed a probabilistic clustering approach based on sampling k-means solutions using AQC. By using all valid measurements, calibrated confidence scores are computed at little cost and solutions are competitive to an iterative balanced k-means approach. We evaluated our method on synthetic as well as real data using simulation, exhaustive search as well as the D-Wave Advantage 2 prototype AQC to explore the potential of quantum computing in machine learning and computer vision.

While the approach is still limited in the problem size, quantum computing enables a fundamentally different approach to clustering that can provide additional information that is costly to compute otherwise. Nevertheless, even with the current progress and potential to scale to real-world problems, more work is required to adapt existing problem formulations, such that the full capability of quantum computing can be effectively used.

Acknowledgments

This work was funded by Toyota Motor Europe via the research project TRACE Zürich.

References

- Amira Abbas, David Sutter, Christa Zoufal, Aurelien Lucchi, Alessio Figalli, and Stefan Woerner. The power of quantum neural networks. *Nature Computational Science*, 1(6):403–409, June 2021. ISSN 2662-8457. doi: 10.1038/s43588-021-00084-1.
- Esma Aïmeur, Gilles Brassard, and Sébastien Gambs. Quantum clustering algorithms. In *Proceedings of the 24th International Conference on Machine Learning - ICML '07*, pp. 1–8, Corvallis, Oregon, 2007. ACM Press. ISBN 978-1-59593-793-3. doi: 10.1145/1273496.1273497.
- Davis Arthur and Prasanna Date. Balanced k-means clustering on an adiabatic quantum computer. *Quantum Information Processing*, 20(9):294, September 2021. ISSN 1573-1332. doi: 10.1007/s11128-021-03240-8.
- M. Benkner, Z. Lahner, V. Golyanik, C. Wunderlich, C. Theobalt, and M. Moeller. Q-match: Iterative shape matching via quantum annealing. In *2021 IEEE/CVF International Conference on Computer Vision (ICCV)*, pp. 7566–7576, Los Alamitos, CA, USA, October 2021. IEEE Computer Society. doi: 10.1109/ICCV48922.2021.00749.
- Marcel Seelbach Benkner, Vladislav Golyanik, Christian Theobalt, and Michael Moeller. Adiabatic Quantum Graph Matching with Permutation Matrix Constraints. In *2020 International Conference on 3D Vision (3DV)*, pp. 583–592, Fukuoka, Japan, November 2020. IEEE. ISBN 978-1-72818-128-8. doi: 10.1109/3DV50981.2020.00068.
- Alex Bewley, Zongyuan Ge, Lionel Ott, Fabio Ramos, and Ben Uppcroft. Simple Online and Realtime Tracking. In *2016 IEEE International Conference on Image Processing (ICIP)*, pp. 3464–3468, September 2016. doi: 10.1109/ICIP.2016.7533003.
- Tolga Birdal, Vladislav Golyanik, Christian Theobalt, and Leonidas Guibas. Quantum Permutation Synchronization. In *2021 IEEE/CVF Conference on Computer Vision and Pattern Recognition (CVPR)*, pp. 13117–13128, Nashville, TN, USA, June 2021. IEEE. ISBN 978-1-66544-509-2. doi: 10.1109/CVPR46437.2021.01292.

-
- M. Born and V. Fock. Beweis des Adiabatsatzes. *Zeitschrift für Physik*, 51(3):165–180, March 1928. ISSN 0044-3328. doi: 10.1007/BF01343193.
- P. I. Bunyk, E. Hoskinson, M. W. Johnson, E. Tolkacheva, F. Altomare, A. J. Berkley, R. Harris, J. P. Hilton, T. Lanting, and J. Whittaker. Architectural considerations in the design of a superconducting quantum annealing processor. *IEEE Transactions on Applied Superconductivity*, 24(4):1–10, August 2014. ISSN 1051-8223, 1558-2515. doi: 10.1109/TASC.2014.2318294.
- Mathilde Caron, Piotr Bojanowski, Armand Joulin, and Matthijs Douze. Deep Clustering for Unsupervised Learning of Visual Features. In *Computer Vision – ECCV 2018*, volume 11218, pp. 139–156. Springer International Publishing, Cham, 2018. ISBN 978-3-030-01263-2. doi: 10.1007/978-3-030-01264-9_9.
- Raúl V. Casaña-Eslava, Paulo J. G. Lisboa, Sandra Ortega-Martorell, Ian H. Jarman, and José D. Martín-Guerrero. A Probabilistic framework for Quantum Clustering, February 2019.
- Raúl V. Casaña-Eslava, Paulo J. G. Lisboa, Sandra Ortega-Martorell, Ian H. Jarman, and José D. Martín-Guerrero. Probabilistic quantum clustering. *Knowledge-Based Systems*, 194:105567, April 2020. ISSN 0950-7051. doi: 10.1016/j.knosys.2020.105567.
- Hsu-kuang Chiu, Jie Li, Rares Ambrus, and Jeannette Bohg. Probabilistic 3D multi-modal, multi-object tracking for autonomous driving. *IEEE International Conference on Robotics and Automation (ICRA)*, 2021.
- Adam Coates and Andrew Y. Ng. Learning Feature Representations with K-Means. In Grégoire Montavon, Geneviève B. Orr, and Klaus-Robert Müller (eds.), *Neural Networks: Tricks of the Trade*, volume 7700, pp. 561–580. Springer Berlin Heidelberg, Berlin, Heidelberg, 2012. ISBN 978-3-642-35288-1. doi: 10.1007/978-3-642-35289-8_30.
- G.B. Coleman and H.C. Andrews. Image segmentation by clustering. *Proceedings of the IEEE*, 67(5):773–785, May 1979. ISSN 1558-2256. doi: 10.1109/PROC.1979.11327.
- D-Wave Systems Inc. Performance advantage in quantum Boltzmann sampling. Technical report, D-Wave Systems Inc., July 2017.
- Prasanna Date, Davis Arthur, and Lauren Pusey-Nazzaro. QUBO formulations for training machine learning models. *Scientific Reports*, 11(1):10029, December 2021. ISSN 2045-2322. doi: 10.1038/s41598-021-89461-4.
- S. Debnath, N. M. Linke, C. Figgatt, K. A. Landsman, K. Wright, and C. Monroe. Demonstration of a small programmable quantum computer with atomic qubits. *Nature*, 536(7614):63–66, August 2016. ISSN 1476-4687. doi: 10.1038/nature18648.
- Nachiket Deo and Mohan M. Trivedi. Multi-Modal Trajectory Prediction of Surrounding Vehicles with Maneuver based LSTMs. In *IEEE Intelligent Vehicles Symposium (IV)*, 2018.
- Nameirakpam Dhanachandra, Khumanthem Manglem, and Yambem Jina Chanu. Image Segmentation Using K - means Clustering Algorithm and Subtractive Clustering Algorithm. *Procedia Computer Science*, 54:764–771, January 2015. ISSN 1877-0509. doi: 10.1016/j.procs.2015.06.090.
- Vivek Dixit, Raja Selvarajan, Muhammad A. Alam, Travis S. Humble, and Sabre Kais. Training Restricted Boltzmann Machines With a D-Wave Quantum Annealer. *Frontiers in Physics*, 9, 2021. ISSN 2296-424X.
- A. Einstein, B. Podolsky, and N. Rosen. Can Quantum-Mechanical Description of Physical Reality Be Considered Complete? *Physical Review*, 47(10):777–780, May 1935. doi: 10.1103/PhysRev.47.777.
- Martin Ester, Hans-Peter Kriegel, Jörg Sander, and Xiaowei Xu. A density-based algorithm for discovering clusters in large spatial databases with noise. In *Proceedings of the Second International Conference on Knowledge Discovery and Data Mining*, KDD’96, pp. 226–231, Portland, Oregon, August 1996. AAAI Press.
- Jeffrey Fisher, Peter Christen, Qing Wang, and Erhard Rahm. A Clustering-Based Framework to Control Block Sizes for Entity Resolution. In *Proceedings of the 21th ACM SIGKDD International Conference on Knowledge Discovery and Data Mining*, KDD ’15, pp. 279–288, New York, NY, USA, August 2015. Association for Computing Machinery. ISBN 978-1-4503-3664-2. doi: 10.1145/2783258.2783396.

-
- R. A. Fisher. The Use of Multiple Measurements in Taxonomic Problems. *Annals of Eugenics*, 7(2):179–188, 1936. ISSN 2050-1439.
- E. Forgy. Cluster Analysis of Multivariate Data: Efficiency versus Interpretability of Classification. *Biometrics*, 21(3):768–769, 1965.
- E. B. Fowlkes and C. L. Mallows. A Method for Comparing Two Hierarchical Clusterings. *Journal of the American Statistical Association*, 78(383):553–569, September 1983. ISSN 0162-1459. doi: 10.1080/01621459.1983.10478008.
- Martin Hirzer, Csaba Beleznaï, Peter M. Roth, and Horst Bischof. Person Re-identification by Descriptive and Discriminative Classification. In Anders Heyden and Fredrik Kahl (eds.), *Image Analysis*, volume 6688, pp. 91–102. Springer Berlin Heidelberg, Berlin, Heidelberg, 2011. ISBN 978-3-642-21226-0. doi: 10.1007/978-3-642-21227-7_9.
- Y.-W. Peter Hong, Lin-Ming Huang, and Hou-Tung Li. Vector Quantization and Clustered Key Mapping for Channel-Based Secret Key Generation. *IEEE Transactions on Information Forensics and Security*, 12(5):1170–1181, May 2017. ISSN 1556-6021. doi: 10.1109/TIFS.2017.2656459.
- David Horn and Assaf Gottlieb. The method of quantum clustering. In T. Dietterich, S. Becker, and Z. Ghahramani (eds.), *Advances in Neural Information Processing Systems*, volume 14. MIT Press, 2001.
- Lawrence Hubert and Phipps Arabie. Comparing partitions. *Journal of Classification*, 2(1):193–218, December 1985. ISSN 1432-1343. doi: 10.1007/BF01908075.
- Ernst Ising. Beitrag zur Theorie des Ferromagnetismus. *Zeitschrift für Physik*, 31(1):253–258, February 1925. ISSN 0044-3328. doi: 10.1007/BF02980577.
- Chiyu “Max” Jiang, Andre Cornman, Cheolho Park, Benjamin Sapp, Yin Zhou, and Dragomir Anguelov. MotionDiffuser: Controllable Multi-Agent Motion Prediction Using Diffusion. In *Proceedings of the IEEE/CVF Conference on Computer Vision and Pattern Recognition*, pp. 9644–9653, 2023.
- Tadashi Kadowaki and Hidetoshi Nishimori. Quantum annealing in the transverse Ising model. *Physical Review E*, 58(5):5355–5363, November 1998. ISSN 1063-651X, 1095-3787. doi: 10.1103/PhysRevE.58.5355.
- Margret Keuper, Siyu Tang, Bjoern Andres, Thomas Brox, and Bernt Schiele. Motion Segmentation & Multiple Object Tracking by Correlation Co-Clustering. *IEEE Transactions on Pattern Analysis and Machine Intelligence*, 42(1):140–153, January 2020. ISSN 0162-8828, 2160-9292, 1939-3539. doi: 10.1109/TPAMI.2018.2876253.
- S. Lazebnik, C. Schmid, and J. Ponce. Beyond Bags of Features: Spatial Pyramid Matching for Recognizing Natural Scene Categories. In *2006 IEEE Computer Society Conference on Computer Vision and Pattern Recognition (CVPR’06)*, volume 2, pp. 2169–2178, June 2006. doi: 10.1109/CVPR.2006.68.
- Ying Liao, Huan Qi, and Weiqun Li. Load-Balanced Clustering Algorithm With Distributed Self-Organization for Wireless Sensor Networks. *IEEE Sensors Journal*, 13(5):1498–1506, May 2013. ISSN 1558-1748. doi: 10.1109/JSEN.2012.2227704.
- S. Lloyd. Least squares quantization in PCM. *IEEE Transactions on Information Theory*, 28(2):129–137, March 1982. ISSN 1557-9654. doi: 10.1109/TIT.1982.1056489.
- Mikko I. Malinen and Pasi Fränti. Balanced K-Means for Clustering. In Pasi Fränti, Gavin Brown, Marco Loog, Francisco Escolano, and Marcello Pelillo (eds.), *Structural, Syntactic, and Statistical Pattern Recognition*, volume 8621, pp. 32–41. Springer Berlin Heidelberg, Berlin, Heidelberg, 2014. ISBN 978-3-662-44414-6. doi: 10.1007/978-3-662-44415-3_4.
- Catherine McGeoch and Pau Farré. The Advantage System: Performance Update. Technical report, D-Wave Systems Inc., October 2021.
- Catherine McGeoch, Pau Farre, and Kelly Boothby. The D-Wave Advantage2 Prototype. *Technical Report*, June 2022.

-
- Samuel Muel, Mario Abad, Miguel Bermejo, Javier Sánchez, Enrique Lizaso, and Román Orús. Hybrid quantum investment optimization with minimal holding period. *Scientific Reports*, 11(1):19587, October 2021. ISSN 2045-2322. doi: 10.1038/s41598-021-98297-x.
- Vikram Khipple Mulligan, Hans Melo, Haley Irene Merritt, Stewart Slocum, Brian D. Weitzner, Andrew M. Watkins, P. Douglas Renfrew, Craig Pelissier, Paramjit S. Arora, and Richard Bonneau. Designing Peptides on a Quantum Computer, March 2020.
- Jon Nelson, Marc Vuffray, Andrey Y. Lokhov, Tameem Albash, and Carleton Coffrin. High-Quality Thermal Gibbs Sampling with Quantum Annealing Hardware. *Physical Review Applied*, 17(4):044046, April 2022. doi: 10.1103/PhysRevApplied.17.044046.
- Florian Neukart, Gabriele Compstella, Christian Seidel, David von Dollen, Sheir Yarkoni, and Bob Parney. Traffic Flow Optimization Using a Quantum Annealer. *Frontiers in ICT*, 4:29, 2017. ISSN 2297-198X. doi: 10.3389/fict.2017.00029.
- Masayuki Ohzeki, Akira Miki, Masamichi J. Miyama, and Masayoshi Terabe. Control of Automated Guided Vehicles Without Collision by Quantum Annealer and Digital Devices. *Frontiers in Computer Science*, 1:9, 2019. ISSN 2624-9898. doi: 10.3389/fcomp.2019.00009.
- Sakrapee Paisitkriangkrai, Chunhua Shen, and Anton Van Den Hengel. Learning to rank in person re-identification with metric ensembles. In *2015 IEEE Conference on Computer Vision and Pattern Recognition (CVPR)*, pp. 1846–1855, Boston, MA, USA, June 2015. IEEE. ISBN 978-1-4673-6964-0. doi: 10.1109/CVPR.2015.7298794.
- Thomas Pochart, Paulin Jacquot, and Joseph Mikael. On the challenges of using D-Wave computers to sample Boltzmann Random Variables, December 2021.
- Andrew Rosenberg and Julia Hirschberg. V-Measure: A Conditional Entropy-Based External Cluster Evaluation Measure. In *Proceedings of the 2007 Joint Conference on Empirical Methods in Natural Language Processing and Computational Natural Language Learning (EMNLP-CoNLL)*, pp. 410–420, Prague, Czech Republic, June 2007. Association for Computational Linguistics.
- E. Schrödinger. Discussion of Probability Relations between Separated Systems. *Mathematical Proceedings of the Cambridge Philosophical Society*, 31(4):555–563, October 1935. ISSN 1469-8064, 0305-0041. doi: 10.1017/S0305004100013554.
- Peter W. Shor. Polynomial-Time Algorithms for Prime Factorization and Discrete Logarithms on a Quantum Computer. *SIAM Review*, 41(2):303–332, January 1999. ISSN 0036-1445. doi: 10.1137/S0036144598347011.
- Mark M. Wilde. *Quantum Information Theory*. Cambridge University Press, Cambridge, 2 edition, 2017. ISBN 978-1-107-17616-4. doi: 10.1017/9781316809976.
- Rui Xu and D. Wunsch. Survey of clustering algorithms. *IEEE Transactions on Neural Networks*, 16(3):645–678, May 2005. ISSN 1941-0093. doi: 10.1109/TNN.2005.845141.
- Jianwei Yang, Devi Parikh, and Dhruv Batra. Joint Unsupervised Learning of Deep Representations and Image Clusters. In *2016 IEEE Conference on Computer Vision and Pattern Recognition (CVPR)*, pp. 5147–5156, Las Vegas, NV, USA, June 2016. IEEE. ISBN 978-1-4673-8851-1. doi: 10.1109/CVPR.2016.556.
- Jan-Nico Zaech, Alexander Liniger, Martin Danelljan, Dengxin Dai, and Luc Van Gool. Adiabatic Quantum Computing for Multi Object Tracking. In *2022 IEEE/CVF Conference on Computer Vision and Pattern Recognition (CVPR)*, pp. 8801–8812, New Orleans, LA, USA, June 2022. IEEE. ISBN 978-1-66546-946-3. doi: 10.1109/CVPR52688.2022.00861.
- Zhedong Zheng, Xiaodong Yang, Zhiding Yu, Liang Zheng, Yi Yang, and Jan Kautz. Joint Discriminative and Generative Learning for Person Re-Identification. In *2019 IEEE/CVF Conference on Computer Vision and Pattern Recognition (CVPR)*, pp. 2133–2142, Long Beach, CA, USA, June 2019. IEEE. ISBN 978-1-72813-293-8. doi: 10.1109/CVPR.2019.00224.